A Discrete Element Stress and Displacement Analysis of Elastoplastic Plates

E. L. STANTON*
McDonnell Douglas Astronautics Company, Western Division, Santa Monica, Calif.
AND
L. A. SCHMIT†
Case Western Reserve University, Cleveland, Ohio

A displacement method of analysis for elastoplastic plates is presented with particular emphasis on accurate stress results. The Hencky-Nadai stress-strain law is assumed and a discretized potential energy function is formed using bicubic Hermite displacement functions. To achieve interelement continuous stress fields, bicubic spline constraints are introduced that produce interelement curvature continuity. The planar variation in material properties caused by plastic strains is approximated using additional nodes that uniformly subdivide the element planform into four quadrants. Integration of the strain energy through the plate thickness is accomplished using gaussian quadrature. Solutions of the nonlinear discretized equilibrium equations are obtained by energy minimization using the conjugate gradient algorithm. Results in the elastic range indicate the displacements converge with the fourth power of the grid size and the stresses converge with the grid size squared. These convergence rates were obtained with both bicubic Hermite and spline displacement functions. Elastoplastic results are presented that compare well with both deformation and incremental theory solutions. Stress results are also presented that demonstrate an elastic compressibility effect in elastoplastic plates.

Introduction

THE present analysis is concerned with the problem of obtaining accurate stress solutions from a discrete element displacement formulation of elastic and plastic plate bending problems. The material is assumed to obey the Hencky-Nadai deformation theory stress-strain law and only active loading is considered. The Illyushin formulation in terms of a plasticity parameter ω (see Fig. 1) is used to derive a plane stress formulation in terms of a new parameter Ω. Bicubic Hermite displacement functions are used to obtain a discrete element idealization of the problem and spline constraints are used to obtain interelement curvature; hence, stress continuity. The in-plane variation in material properties caused by strains in the plastic range is approximated by using additional nodes at midside and at the element center to interpolate these properties. This provides increased accuracy in the integration of the plastic strains without increasing the number of displacement degrees of freedom. The integration of the plastic strains through the plate thickness is accomplished using gaussian quadrature.

The solution of the equilibrium equations is approached as an energy minimization problem using the conjugate gradient algorithm. Since the gradient of the potential energy can be computed element by element without recourse to an assembled stiffness matrix,[1] this approach offers important computational advantages. The diagonal scaling proposed by Fox and Stanton[2] is used and a modification to account for the presence of spline constraints is suggested. A study of stress and displacement convergence rates is made using successively finer uniform grid idealizations of a simply supported plate. To provide comparisons in the elastoplastic range, an early deformation theory solution by Illyushin[3] and a recent incremental theory solution by Armen, Pifko, and Levine[4] are used. The material behaviors assumed in Refs. 3 and 4 are, respectively, linear strain hardening and elastic-perfectly plastic. Results are also presented to illustrate the influence of elastic compressibility on elastoplastic stress distributions.

Potential Function for a Hencky-Nadai Material

Deformation theories of plasticity have been the subject of a continuing discussion among theoreticians for many years because there exist certain path-dependent phenomena that these theories cannot describe.[5] The fundamental assumption regarding material behavior made by a deformation theory is that the total plastic strain ϵ_{ij}^p is uniquely determined by the current state of stress

$$\epsilon_{ij}^p = \epsilon_{ij}^p(\sigma_{ij}) \text{ for } i,j = 1,2,3 \quad (1)$$

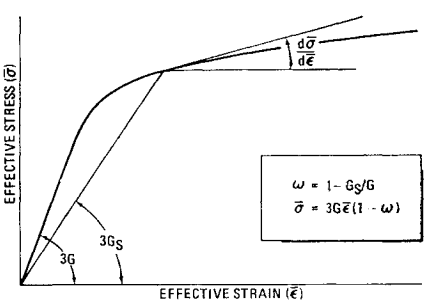

Fig. 1 Effective stress—effective strain diagram.

Received June 17, 1969; revision received January 9, 1970. Portions of this research were supported by the Air Force Flight Dynamics Laboratory, Wright-Patterson AFB, Ohio, under Contract AF 33(615)-3432 at Case Western Reserve University and by McDonnell Douglas Astronautics Company, Western Division Independent Research and Development funds.

* Senior Engineer, Advance Structures and Mechanical Department. Formerly NSF Fellow, Case Western Reserve University.

† Wilbert J. Austin Professor of Engineering; currently Professor of Engineering, University of California at Los Angeles. Associate Fellow AIAA.

Accepting Drucker's material stability postulates[6] and the notion of a loading surface in stress space, there are definite restrictions on the admissible loading paths for which Eq. (1) can be justified. However, by utilizing a singularity or corner in the loading surface at the point of loading (c.f. Ref. 7, p. 104), Budiansky[8] and others have shown that the class of admissible loading paths is considerably wider than just proportional loading. Active‡ loading of many isotropic materials falls in this category and computational tests are available for a posteriori numerical verification of admissibility. Most applications of deformation theories, including the present, are of the active loading type.

The most widely used of the deformation theories is the Hencky-Nadai or secant modulus theory based on the von Mises yield criteria

$$\epsilon_{ij}{}^{p} = \tfrac{3}{2}(\bar{\epsilon}^{p}/\bar{\sigma})s_{ij} \text{ for } i,j = 1,2,3 \tag{2}$$

where the deviatoric stress tensor s_{ij}, the effective stress $\bar{\sigma}$, and the effective plastic strain $\bar{\epsilon}^{p}$ are

$$s_{ij} = \sigma_{ij} - \tfrac{1}{3}\sigma_{kk}\delta_{ij} \tag{2a}$$

$$\bar{\sigma} = (\tfrac{3}{2}s_{ij}s_{ij})^{1/2} \tag{2b}$$

$$\bar{\epsilon}^{p} = (\tfrac{2}{3}\epsilon_{ij}{}^{p}\epsilon_{ij}{}^{p})^{1/2} \tag{2c}$$

and δ_{ij} is Kronecker's delta. Introducing the bulk modulus K, the coefficient of thermal expansion α and a temperature distribution T; the stress-strain law in terms of Illyushin's[3] plasticity parameter $\omega(\omega = 1 - G_s/G = \bar{\epsilon}^{p}/\bar{\epsilon})$ is, for uncoupled temperature effects,

$$\sigma_{ij} = 2G(1-\omega)(\epsilon_{ij} - \tfrac{1}{3}\epsilon_{kk}\delta_{ij}) - 3K(\alpha T - \tfrac{1}{3}\epsilon_{kk})\delta_{ij} \quad \text{for } i,j,k = 1,2,3 \tag{3}$$§

which can be written as

$$s_{ij} = 2G_s e_{ij} \text{ for } i,j = 1,2,3 \tag{4}$$

using the secant modulus G_s and the stress and strain deviators s_{ij} and e_{ij}. The relation between the strain deviator e_{ij} and the strain ϵ_{ij} is analogous to Eq. (2a). The form of the strain energy density $W(\epsilon_{ij})$ given by Illyushin is

$$W(\epsilon_{ij}) = \int_0^{\bar{\epsilon}} \bar{\sigma}(\eta)d\eta + \frac{1}{2}K(\epsilon_{kk})^2 - 3K\alpha T\epsilon_{kk} \tag{5}$$

which is compact and conceptually clear but does not lend itself readily to discrete element approximation. The Hemholtz free-energy functional

$$W(\epsilon_{ij}) = \int_0^{\epsilon_{ij}} \sigma_{ij}(\eta_{ij})d(\eta_{ij} - \alpha T\delta_{ij}) \tag{6}$$

and Eq. (3) after partial integration give

$$W(\epsilon_{ij}) = \int_0^{\epsilon_{ij}\epsilon_{ij}} G(1-\omega)d\eta_{ij} + \frac{1}{2}\int_0^{(\epsilon_{kk})^2}\left[K - \frac{2}{3}G(1-\omega)\right]d\eta_{kk} - 3K\alpha T\epsilon_{kk} \tag{7}$$

omitting a constant of integration. Actually to evaluate Eq. (7) requires a specific stress-strain diagram that defines $\omega(\bar{\epsilon})$. However, the equilibrium equations depend only on the first variation of $W(\epsilon_{ij})$ and the discretized equilibrium equations can be formed using Leibnitz's rule without first specifying any particular material stress-strain diagram. When an energy search procedure is used to solve the nonlinear equilibrium equations, however, it may be necessary to evaluate $W(\epsilon_{ij})$ in addition to forming the equilibrium equations. Actually the energy search only strictly requires the value of some function $W^*(\epsilon_{ij})$ consistent¶ with $W(\epsilon_{ij})$. The readily computed function

$$\begin{aligned} W^*(\epsilon_{ij}) &= G(1-\omega)\epsilon_{ij}\epsilon_{ij} + \tfrac{1}{2}[K - \tfrac{2}{3}G(1-\omega)] \times (\epsilon_{kk})^2 - 3K\alpha T\epsilon_{kk} \\ &= G(1-\omega)e_{ij}e_{ij} + \tfrac{1}{2}K(\epsilon_{kk})^2 - 3K\alpha T\epsilon_{kk} \end{aligned} \tag{8}$$

can be written as

$$W^*(\epsilon_{ij}) = \tfrac{1}{2}\bar{\sigma}(\bar{\epsilon})\bar{\epsilon} + \tfrac{1}{2}K(\epsilon_{kk})^2 - 3K\alpha T\epsilon_{kk} \tag{9}$$

using Eqs. (2b), (4), and $\bar{\sigma} = 3G\bar{\epsilon}(1-\omega)$, and the conditions $\bar{\sigma}, \bar{\epsilon} > 0$; $0 \leq d\bar{\sigma}/d\bar{\epsilon} < \infty$ can be used to show that $W^*(\epsilon_{ij})$ is consistent with $W(\epsilon_{ij})$. It should also be noted that the first variation of Eq. (7) can be obtained from Eq. (8) if ω is considered constant during the variation. This procedure is used by Havner[9] to derive finite difference equilibrium equations. The introduction of $W^*(\epsilon_{ij})$ in the present case is strictly for computational ease in the energy search and is not required in the discrete element approach.

The strain energy density expressed in terms of displacements $W(U_k) \equiv W[\epsilon_{ij}(U_k)]$ can now be used to write the potential energy function

$$\Pi(U_k) = \int_V W(U_k)dV - \int_V B_k U_k dV - \int_S X_k U_k ds \tag{10}$$

where S is that portion of the boundary of V on which tractions X_k are prescribed, and B_k are the body forces. A proof of the minimum potential energy theorem for a stable Hencky-Nadai material is given by Illyushin[3] using the principle of virtual work and $d\bar{\sigma}/d\bar{\epsilon} \geq 0$. Since W^* is consistent with W, the function Π^* obtained by substituting W^* in Eq. (10) is consistent with Π in the sense previously defined.

A Plane Stress Formulation

A formulation that isolates the effect of elastic compressibility is presented for the study of plate bending. Thermal stresses will not be considered; however, this same formulation including temperature effects may be found in Ref. 10. Using the plane stress assumption $\sigma_{33} = 0$ in Eq. (3) gives

$$\epsilon_{33} = -(1-3\Omega)(\epsilon_{11} + \epsilon_{22}),\ \epsilon_{kk} = 3\Omega(\epsilon_{11} + \epsilon_{22}) \tag{11}$$

where

$$\Omega \equiv [(1-2\nu)(1-\omega)]/[3(1-\nu) - 2\omega(1-2\nu)] \tag{12}$$

and ν is the elastic Poisson ratio. The limiting conditions of elastic incompressibility ($\nu = \frac{1}{2}$) and infinite strain in a material with a perfectly plastic asymptote ($\omega = 1$) both result in Ω being zero. Substituting the remaining plane stress assumptions $\sigma_{13} = \sigma_{23} = 0$ in Eq. (8) gives

$$W^*(\epsilon_{ij}) = 2G(1-\omega)(\epsilon_{11}{}^2 + \epsilon_{11}\epsilon_{22} + \epsilon_{22}{}^2 + \epsilon_{12}{}^2) - 3G(1-\omega)\Omega(\epsilon_{11} + \epsilon_{22})^2 \tag{13}$$

where the associated stress-strain equations are

$$\begin{aligned} \sigma_{11} &= 2G(1-\omega)[\epsilon_{11} + (1-3\Omega)(\epsilon_{11} + \epsilon_{22})] \\ \sigma_{22} &= 2G(1-\omega)[\epsilon_{22} + (1-3\Omega)(\epsilon_{11} + \epsilon_{22})] \\ \sigma_{12} &= 2G(1-\omega)\epsilon_{12} \end{aligned} \tag{14}$$

This formulation offers some qualitative insight into the influence of elastic compressibility in the plastic range. The maximum possible value of $\Omega(\omega,\nu)$ is $\Omega(0,0) = \frac{1}{3}$ and a graph of this function (c.f. Ref. 10, p. 85) for fixed ν will show that initially, for small plastic strains, Ω changes slowly. [In fact, $G(1-\omega)\Omega$ is approximately linear in ω for, say, $0 \leq \omega \leq 0.3$.] Thus, the importance of elastic compressibility for plastic plane stress problems remains

‡ Active in the sense that the effective stress $\bar{\sigma}$ and effective strain $\bar{\epsilon}$ are monotonic with load.

§ The usual summation convention of Cartesian tensor calculus for repeated Latin indices is adopted.

¶ The term consistent is used here to imply that the equalities and inequalities of $W(\epsilon_{ij})$ are preserved in $W^*(\epsilon_{ij})$.

basically the same as in the elastic range until rather high strain levels are reached. After this they rapidly decrease approaching zero for materials that become perfectly plastic in the limit ($\omega = 1$).

Discrete Element Displacement Functions

The formulation of discrete displacement functions is very often a heuristic proposition with no guarantee that the global displacement function, which results from linking the individual elements, satisfies the admissibility conditions of the variational problem. Even when the implied global displacement function is admissible there is usually no guarantee that the discrete element grid is energy complete.[11] Melosh[12] recognized this situation clearly and serious efforts have been made to define conditions on the local or element displacement functions sufficient to guarantee admissibility and energy completeness. Considering admissibility first, Schmit[13] and Pian[14] have given sufficient conditions for membrane and thin-shell elements that require that the displacements be continuous along a common edge and that, in the case of shells, the normal derivative of the lateral displacement must also be continuous along a common edge. Bogner[1] provides an excellent discussion of this topic and shows that element displacement functions based on two-point Hermite interpolation polynomials can be found that satisfy interelement admissibility. The two-point Hermite polynomials are uniquely defined by

$$(d^p/dx^p)H_{ki}^{(N)}(x_q) = \delta_{pk}\delta_{iq} \text{ for } i,q = 1,2 \quad p,k = 0,1,\ldots,N \tag{15}$$

which represents $2N + 1$ independent linear conditions that are satisfied by the $2N + 1$ degree polynomial $H_{ki}^{(N)}(x)$. The element displacement functions are then formed using the bivariate Hermite interpolation formula

$$f(x,y) \doteq f^{(N)}(x,y) = \sum_{i=1}^{2}\sum_{j=1}^{2}\sum_{k=0}^{N}\sum_{l=0}^{N} \times H_{ki}^{(N)}(x)H_{lj}^{(N)}(y)\frac{\partial^{k+l}}{\partial x^k \partial y^l} f(x_i,y_j) \tag{16}$$

In the present case, the bicubic ($N = 1$) form of Eq. (16) has been used as in Ref. 1.

The question of energy completeness or finite element completeness as McLay[15] refers to it, or relative completeness as Kantorovich and Krylov[16] refer to it, is basically a question of interpolation error. Is it possible to interpolate the admissible displacement functions and all of their derivatives appearing in the energy functional with arbitrarily small error? The local nature of the element displacement functions causes this to be a problem in piecewise polynomial approximation. In a recent paper by Birkhoff, Schultz, and Varga[17] sharp error bounds for piecewise Hermite interpolation were obtained that answer the energy completeness question for elements based on these functions when the structure is a rectangular polygon. Let ρ represent a particular idealization of the structure R and let C be a collection of idealizations $\rho \epsilon C$. Such a collection is said to be regular if the aspect ratio $(a/b)_i$ of every element in every ρ is bounded above and below by constants independent of the particular idealization. Let $U_\rho^{(N)}$ be the bivariate Hermite interpolate of an admissible displacement function U obtained by linking the elements of the idealization ρ. Then defining $\Delta \equiv \max b_i$ and assuming U is sufficiently differentiable there exists a constant M such that (c.f. Ref. 17, Definition 8, Theorem 6)

$$||[(\partial^{k+l})/\partial x^k \partial y^l][U - U_\rho^{(N)}]||_{L^r(R)} \leqslant M(\Delta)^{2N+2-k-l} \tag{17}$$

for all $\rho \epsilon C$

and for all $0 < k, l < N + 1$ with $0 < k + l < 2N + 1$. If the energy is minimized over these functions where N is chosen to satisfy admissibility then the true minimum energy is approached as Δ approaches zero. It should be emphasized that Eq. (17) is an error bound for interpolation and not the variational problem. To obtain the latter most investigators in mechanics use the energy norm (c.f. Ref. 11, p. 52) while for elliptic problems Birkhoff, Schultz, and Varga use Sobolev norms (c.f. Ref. 17, p. 249). The basic property needed is that the solution of the finite dimensional or Ritz problem is closer in these norms to the true solution than any other function in the subspace. Since this is true of every function in the subspace, it is true in particular for the interpolate of the exact solution. Now error bounds established for interpolation can be used to give error bounds for the variational problem with the aid of certain inequalities between norms. The mathematics of this procedure may be found in Ref. 17.

Formulation of the Element Matrices

In linear and geometrically nonlinear problems the element stiffness matrices can be determined permanently once the assumed displacement functions are substituted into the potential energy and integrated. This is no longer true when the material properties are nonlinear although some measure of permanence can be retained by using interpolatory quadrature for the material properties. Ideally the quadrature used for the material properties should be consistent with the assumed displacement functions. Herbold[18] provides a thorough analysis of this question and indicates several quadrature schemes for the nonlinear Dirichlet problem that are consistent with bicubic Hermite and bicubic spline functions. Unfortunately these schemes require that the volume integrations be remade at every step in the iterative solution of the nonlinear equilibrium equations. The present approach does just this for the integration through the thickness but uses five additional nodes to interpolate the material properties in the plane for the area integration. These nodes subdivide the element into four congruent areas and then bilinear Hermite interpolation is used in each. Invoking intraelement continuity, this amounts to a nine-parameter interpolation instead of the analogous four-parameter interpolation used by Armen, Pifko, and Levine.[4] Referring to Eq. (17) the relative improvement in the material properties is a factor of four without introducing additional displacement degrees of freedom. The strain displacement equations of small deflection plate theory using the conventional x,y,z,W notation

$$\epsilon_x = -zW_{,xx}; \quad \epsilon_y = -zW_{,yy}; \quad \epsilon_{xy} = -zW_{,xy} \tag{18}**$$

when substituted into the potential energy expression yield

$$\Pi^* = \tfrac{1}{2}\int_A 4GC_1(W_{,xx}^2 + W_{,xx}W_{,yy} + W_{,yy}^2 + W_{,xy}^2)dA - \tfrac{1}{2}\int_A 6GC_2(W_{,xx} + W_{,yy})^2 dA - \int_A X_z W dA \tag{19}$$

where

$$C_1 = \int_{-(h/2)}^{(h/2)} (1 - \omega)z^2 dz \qquad C_2 = \int_{-(h/2)}^{(h/2)} (1 - \omega)\Omega z^2 dz \tag{20}$$

A convenient vector notation for Eq. (16)

$$W(x,y) = X^T p(x,y)$$

introduced by Bogner[1] will be used to define the discretized form of Eq. (19). The components of $p(x,y)$ are of the form

** The comma notation denotes differentiation with respect to the coordinate variables indicated by subscripts to the right of the comma.

$H_{ki}^{(1)}(x)H_{lj}^{(1)}(y)$ and are listed in Ref. 10 along with the nodal parameters W_{11}, $W_{11,x}$, etc., in the vector X. The discretized form of Eq. (20) is left in summation form to indicate the distinctly different manner in which it enters the element matrices

$$C_1 = \sum_{i=1}^{9} g_i(x,y) \int_{-(h/2)}^{(h/2)} [1 - \omega(x_i,y_i,z)]z^2dz = \sum_{i=1}^{9} \zeta_i g_i(x,y) \tag{21}$$

$$C_2 = \sum_{i=1}^{9} g_i(x,y) \int_{-h/2}^{h/2} [1 - \omega(x_i,y_iz)]\Omega(x_i,y_i,z)z^2dz = \sum_{i=1}^{9} \eta_i g_i(x,y)$$

The functions $g_i(x,y)$ are locally bilinear Hermite polynomials of the form $H_{ki}^{(0)}(x)H_{lj}^{(0)}(y)$ in each of the four quadrants of the element and are defined explicitly in Ref. 10. The discretized form of Eq. (19) can now be written

$$\Pi^* = \Pi^*(X) = \tfrac{1}{2}X^TK_\omega X - \tfrac{1}{2}X^TQ_\omega X - X^TF \tag{22}$$

where

$$K_\omega = 4G\int_A \sum_{i=1}^{9} \zeta_i g_i(x,y)[p_{,xx}p_{,xx}^T + \frac{1}{2}(p_{,xx}p_{,yy}^T + p_{,yy}p_{,xx}^T) + p_{,yy}p_{,yy}^T + p_{,xy}p_{,xy}^T]dA$$

$$Q_\omega = 6G\int_A \sum_{i=1}^{9} \eta_i g_i(x,y)[p_{,xx}p_{,xx}^T + p_{,xx}p_{,yy}^T + p_{,yy}p_{,xx}^T + p_{,yy}p_{,yy}^T]dA \tag{23}$$

The linear strain displacement assumptions of Eq. (18) do not in general permit a simple analytic integration for C_1 and C_2 since $\epsilon_z = [\Omega(\omega,\nu) - \frac{1}{3}](\epsilon_x + \epsilon_y)$ is a nonlinear equation for any z in the plastic zone. The only exception occurs with an elastically incompressible material when $\Omega(\omega, \frac{1}{2}) \equiv 0$. Illyushin[3] used this simplifying assumption ($\nu = \frac{1}{2}$) to great advantage in obtaining precomputer solutions. A slightly weaker assumption, equivalent to Ω being a nonzero constant, was used recently by Ohashi and Kamiya[19] with excellent results for the circular plate problem. After consideration of these and other integration schemes, gaussian quadrature was selected for Eq. (21). It requires no simplifying assumptions about material behavior and it is capable of great precision with few integration points. Normalizing the interval by the change of variables $\xi = 2z/h$ and using symmetry about $\xi = 0$ gives

$$\zeta_i = \frac{h^3}{4}\sum_{k=1}^{3} \lambda_k^{(7)}[1 - \omega(x_i,y_i,\xi_k^{(7)})](\xi_k^{(7)})^2 \tag{24}$$

for seven-point gaussian quadrature with an analogous expression for η_i. The Christoffel numbers $\lambda_k^{(7)}$ and integration points $\xi_k^{(7)}$ for a unit weight function on $[-1,1]$ are tabulated in several mathematical handbooks.

The bicubic Hermite displacement functions from Eq. (16) with $N = 1$ can produce an approximate displacement field $W_\rho^{(1)}$, that is, at most $C^{(1)}$

$$[(\partial^{k+l})/\partial x^k dy^l]W_\rho^{(1)} \epsilon C^{(0)} \qquad 0 \leqslant k,l \leqslant 1 \tag{25}$$

However, the error bound in Eq. (17) guarantees that the second derivatives $W_{,xx}$ and $W_{,yy}$ are approximated to within an error of order Δ^2 even though neither is interpolated. Thus, the bending strains can be approximated with $W_\rho^{(1)}$ displacement functions and it is natural to ask if interelement strain continuity would improve on this result for bicubic functions. If higher degree functions (e.g., biquintic Hermite) were used to obtain $C^{(2)}$ displacements the answer is, of course, yes but at the expense of several added degrees of freedom. The bicubic spline functions are $C^{(2)}$, and De Boor[20] has shown that these functions $\overline{W}_\rho^{(1)}$ may be obtained using equality constraints among the nodal parameters of $W_\rho^{(1)}$. The analysis of these functions by Birkhoff and De Boor[21] indicates the same order interpolation error, and the results of Herbold[18] for variational problems show the error is again the same order if consistent quadrature schemes are used. To stay within the confines of the discrete element matrix format in the present analysis a quadrature scheme for material properties was used that is not consistent.†† Several solutions are presented later to investigate what effect if any this has on the relative accuracy of the stresses obtained from $\overline{W}_\rho^{(1)}$ and $W_\rho^{(1)}$.

To indicate briefly the relationship between $\overline{W}_\rho^{(1)}$ and W_ρ^1, define partitions in the coordinate directions x and y of a rectangle by

$$x_0 < x_1 < \ldots < x_{N_x+1} = a$$
$$y_0 < y_1 < \ldots < y_{N_y+1} = b \tag{26}$$

then for type I splines $\overline{W}_\rho^{(1)}$ is uniquely determined by

$$\begin{aligned} &W_{,x}(x_i,y_i) && 1 \leqslant j \leqslant N_y;\ i = O,N_x+1 \\ &W_{,y}(x_i,y_i) && 1 \leqslant i \leqslant N_x;\ j = O,N_y+1 \\ &W(x_i,y_i) && 0 \leqslant i \leqslant N_x+1;\ 0 \leq j \leq N_y+1 \\ &W_{,xy}(x_i,y_i) && i = O,N_x+1;\ j = O,N_y+1 \end{aligned} \tag{27a}$$

The above nodal parameters are the independent degrees of freedom in $\overline{W}_\rho^{(1)}$ from $W_\rho^{(1)}$ with the remaining nodal parameters determined by the equations

$$W_{,x}(x_{i-1},y_j)\Delta x_i + 2W_{,x}(x_i,y_j)[\Delta x_{i-1} + \Delta x_i] + W_{,x}(x_{i+1},y_j)\Delta x_{i-1} = 3\{(\Delta x_{i-1}/\Delta x_i)[W(x_{i+1},y_j) - W(x_i,y_j)] + (\Delta x_i/\Delta x_{i-1})[W(x_i,y_i) - W(x_{i-1},y_j)]\} \tag{27b}$$

for $i = 1,2,\ldots,N_x$ and $j = 0,1,\ldots,N_y+1$

$$W_{,xy}(x_{i-1},y_j)\Delta x_i + 2W_{,xy}(x_i,y_j)[\Delta x_{i-1} + \Delta x_i] + W_{,xy}(x_{i+1},y_j)\Delta x_{i-1} = 3\{(\Delta x_{i-1}/\Delta x_i) \times [W_y(x_{i+1},y_j) - W_{,y}(x_i,y_j)] + (\Delta x_i/\Delta x_{i-1})[W_{,y}(x_i,y_j) - W_{,y}(x_{i-1},y_j)]\} \tag{27c}$$

for $i = 1,2,\ldots,N_x$ and $j = 0,N_y+1$

$$W_{,xy}(x_i,y_{j-1})\Delta y_j + 2W_{,xy}(x_i,y_j)[\Delta y_{j-1} + \Delta y_j] + W_{,xy}(x_i,y_{j+1})\Delta y_{j-1} = 3\{(\Delta y_{j-1}/\Delta y_j)[W_{,x}(x_i,y_{j+1}) - W_{,x}(x_i,y_j)] + (\Delta y_j/\Delta y_{j-1})[W_{,x}(x_i,y_j) - W_{,x}(x_i,y_{j-1})]\}$$

for $i = 0,1,\ldots,N_x+1$ and $j = 1,2,\ldots,N_y$

where $\Delta x_i = x_{i+1} - x_i$ and $\Delta y_j = y_{j+1} - y_j$ (27d)

The equations for $W_{,y}$ may be obtained from Eq. (27b) by reversing the roles of x and y.

Solving the Nonlinear Equilibrium Equations by Energy Search

The energy search method attempts to find the displacement state satisfying equilibrium by treating the potential energy minimization as a mathematical programing problem. After some early work with relaxation type direct methods most recent efforts have used gradient minimization algorithms. Since the gradient of the potential energy

†† The use of bicubic material property interpolation poses subtle mathematical difficulties[18] as well as computational problems.[10]

Table 1 Elastic simply supported plate comparisons for Hermite and spline displacement functions

Grid	N	π^*	W_{max}	Λ_w	$\sigma_{x\ max}$	$\Lambda_{\sigma x}$	$\sigma_{xy\ max}$	$\Lambda_{\sigma xy}$
			Linear elastic bicubic Hermite solution					
1 × 1	4	−0.210733	0.0412270		3432.1		−2003.7	
2 × 2	16	−0.212620	0.0406533	4.4	2953.0	1.5	−1960.5	2.3
3 × 3	36	−0.212772	0.0406291	4.1	2904.1	1.7	−1953.9	2.1
4 × 4	64	−0.212800	0.0406253	4.1	2889.7	1.8	−1951.7	2.
5 × 5	100	−0.212808	0.0406242	4.0	2883.5	1.9	−1950.7	2.00
			Linear elastic bicubic spline solution					
1 × 1	4	−0.210733	0.0412270		3432.1		−2004.7	
2 × 2	9	−0.212581	0.0406447	4.8	2917.6	1.4	−1963.6	1.9
3 × 3	16	−0.212767	0.0406281	3.8	2900.3	1.8	−1955.6	1.9
4 × 4	25	−0.212799	0.0406251	3.8	2888.2	1.9	−1952.7	2.0
5 × 5	36	−0.212808	0.0406242	3.9	2882.9	1.9	−1951.4	2.0
	Reference[a]		0.0406235	...	2873.2	...	−1948.9	...

[a] Navier solution: summed to $M = N = 1503$ in double precision on the CDC 6600.

corresponds directly to the equilibrium equations, these methods are equivalent to a semi-iterative solution for linear equilibrium equations and to an iterative solution for nonlinear ones. Using the variable correlation table[1] or integer map representation of the geometric admissibility conditions, the gradient can be computed element by element without recourse to an assembled stiffness matrix which greatly reduces computer storage requirements. A more complete discussion of gradient methods in structural analysis including the influence of scale effects may be found in Ref. 22.

The two most widely used algorithms are the variable metric and conjugate gradient methods. If the initial step each takes is in the direction of steepest descent, these two algorithms generate the same search directions for quadratic functions;[23] however, in actual computations round off error causes them to differ for all but the most well-conditioned functions.[2] The present solutions were obtained using the conjugate gradient algorithm which minimizes the discretized energy $\Pi(X)$ using the following sequence of directions:

$$\begin{aligned} P_0 &= -\nabla\Pi(X_0) \\ X_{i+1} &= X_i + t_i P_i \\ P_{i+1} &= -\nabla\Pi(X_{i+1}) + \beta_i P_i \end{aligned} \tag{28}$$

where X_0 is any initial guess. The scalar t_i is the smallest positive root of the directional derivative

$$d\Pi(t) = P_i{}^T \nabla\Pi(X_i + tP_i) \tag{29}$$

for prescribed X_i and P_i and thus corresponds to the first minimum of $\Pi(X_i + tP_i)$ on $0 < t$. The scalar β_i is given by

$$\beta_i = \nabla\Pi(X_{i+1})^T \nabla\Pi(X_{i+1}) / \nabla\Pi(X_i)^T \nabla\Pi(X_i) \tag{30}$$

and conditions on the function $\Pi(X)$ sufficient for convergence in nonlinear problems are given in Ref. 24. The scaling transformations used are based on linear elastic stiffness matrices after Ref. 2 and it is important to change scaling transformations when working in the spline subspace of the Hermite variables. To be specific, let K_H be the assembled Hermite stiffness matrix and let T_s be the transformation matrix for Eqs. (27b–d) that takes an M dimensional vector of spline variables into an N dimensional vector ($M \leq N$) of Hermite variables. Then the Hermite scaling should be based on K_H and the spline scaling on $K_s = T_s{}^T K_H T_s$ where the diagonal elements of K_H and K_s can both be computed using the integer map approach without assembling either K_H or K_s.

Numerical Results

The properties of bivariate Hermite and bivariate spline functions described earlier indicate higher-order convergence rates are possible for both stress and displacement. Stress convergence is a direct consequence of the fact that these functions accurately approximate the derivatives of the displacement field. This includes the $N = 1$ bicubic Hermite case even though stress continuity is not maintained, and it is interesting to compare these solutions with the stress continuous bicubic spline results. To determine convergence rates experimentally, let ρ_n denote a square element idealization that partitions a quadrant of the plate with $N_{xn} = N_{yn} = n - 1$. Assuming $\|f - f_{\rho n}{}^{(N)}\|_{L^\infty} = M(\Delta_n)^\Lambda$, the exponent Λ can be computed from successive grid refinements ($n = 1,2, \ldots$) using logarithmic ratios.[18] Similar experiments for the Dirichlet problem by Herbold indicate convergence rates for the variational problem that are very close to the exponents for interpolation error. A linear elastic simply supported plate $10 \times 10 \times 0.1$ in. thick, $\nu = 0.3$, $E = 10.92 \times 10^6$ psi and loaded by a uniform pressure of 1.0 psi is used in these computations. The results shown in Table 1 indicate the stresses converge with Δ^2 and the displacements with Δ^4 for both Hermite and spline solutions which also coincides with the interpolation error exponents. Similar results were also obtained for clamped boundary conditions; and to illustrate the nature of the Hermite solution stress discontinuities, $\sigma_x(x, b/2)$ is plotted in Fig. 2 for several grid refinements of the clamped plate problem. As can be

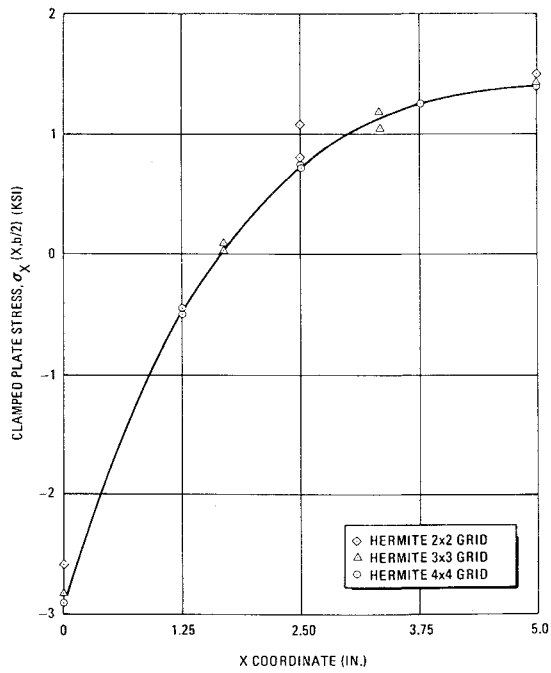

Fig. 2 Interelement mean stress convergence for Hermite displacement functions.

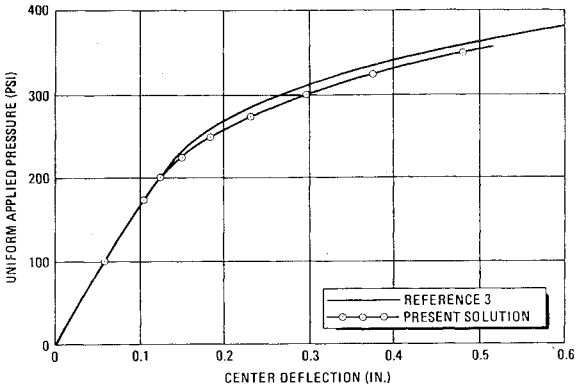

Fig. 3 Simply supported plate load deflection comparisons.

seen the discontinuities become vanishingly small with average value rapidly converging to the true solution. Even smaller discontinuities occur with simply supported boundary conditions.

The early elastoplastic plate bending analyses of Illyushin[3] were based on a deformation theory and used the simplifying assumption of elastic incompressibility. This assumption can lead to stress errors in the corners of a simply supported elastic plate and this behavior continues well into the plastic range. To verify the present analysis first and then investigate this elastic compressibility effect, a simply supported plate is loaded well into the plastic range and analyzed for $\nu = 0.5$ and $\nu = 0.3$. Load deflection comparisons with Ref. 3 for the $\nu = 0.5$ case are shown in Fig. 3 for a linear strain hardening plate $10 \times 10 \times 0.4$ in. thick with $E = 10^7$ psi, $(\frac{1}{3}G)(d\bar{\sigma}/d\bar{\epsilon}) = 0.1$ for $\bar{\sigma} > \sigma_0$ and with a yield stress of $\sigma_0 = 30$ ksi. The agreement is remarkable considering that only one degree of freedom was used to obtain the earlier precomputer solution. To illustrate the stress changes caused by elastic compressibility, comparisons of the effective stress $\bar{\sigma}$ are made in Fig. 4 along one edge of the plate at a load of 250 psi. These comparisons show that the mean stress

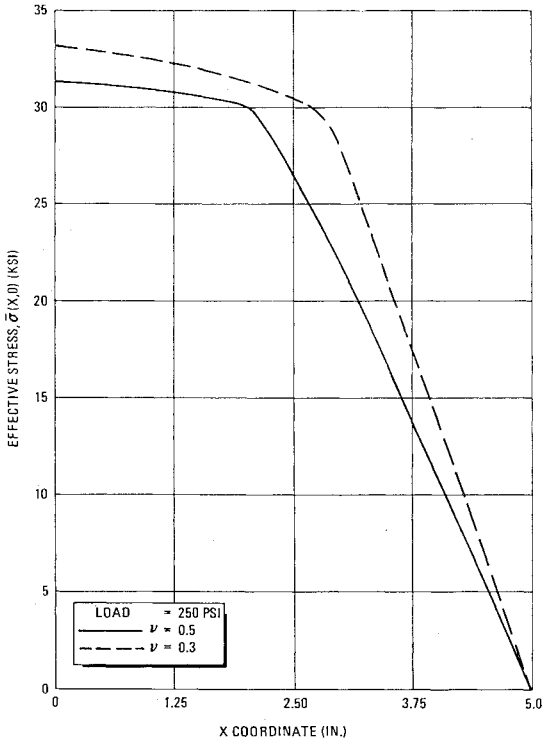

Fig. 4 Influence of elastic compressibility on effective stress.

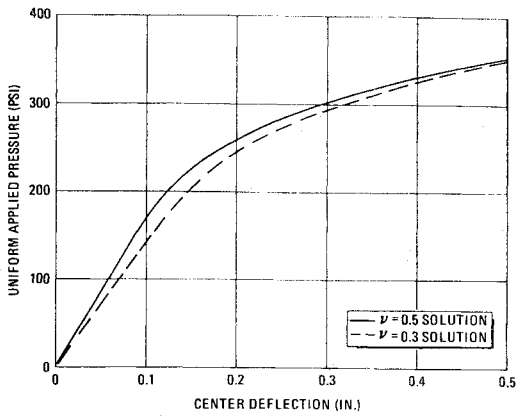

Fig. 5 Influence of elastic compressibility on load deflection.

differences are on the order of 5% except near the elastic boundary where locally higher differences occur. The influence of elastic compressibility on displacements is shown in Fig. 5 and indicates that the $\nu = 0.3$ displacements approach those for $\nu = 0.5$ at high load levels. Similar behavior for an aluminum circular plate was obtained by Ohashi and Kamiya.[19]

Convergence with grid refinement for these nonlinear problems is shown in Table 2 for the $\nu = 0.3$ case at a load of 250 psi. This load produces substantial plastic regions and causes the material property quadrature to strongly influence convergence rates. Unfortunately there is no reference solution that can be used to compute Λ's; however, the fact that the maximum deflection changes in the third place between the 3×3 and 4×4 grid solutions is graphic evidence of slower convergence. This does not preclude accurate solutions, of course, but it does detract from the potential accuracy possible from a given grid with consistent material property quadrature. As a practical matter the added computational expense necessary to realize this potential does not seem justified in general. Comparisons with the Armen, Pifko, and Levine incremental solution for an elastic-perfectly plastic plate (c.f. Fig. 6) show small differences at high load levels. These are on the order of the differences with the Illyushin solution of the previous problem. The present results use a 3×3 grid taking advantage of the additional nodes used in the intraelement material property interpolation to obtain the equivalent of a 6×6 grid for this quadrature. Selected load levels were rerun with finer grids to confirm convergence. The small differences with the Armen, Pifko, and Levine solution could be the result of their linearizing the equilibrium equations each load increment as much as the result of differences in plasticity theory. No stress results are available from Ref. 4; however, stress comparisons with an incremental theory solution in Ref. 10 show good agreement at the plate center.

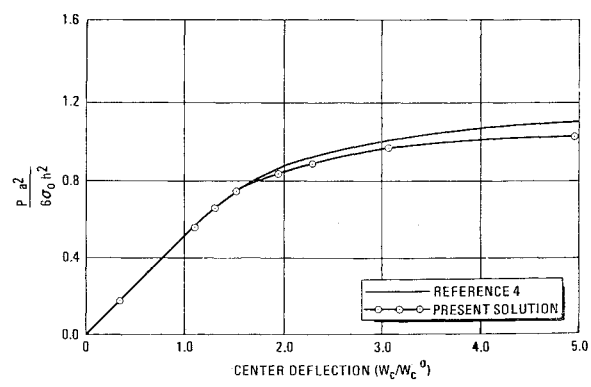

Fig. 6 Armen-Pifko-Levine load deflection comparisons.

Table 2 Elastoplastic simply supported plate comparisons for Hermite and spline displacement functions

Grid	N	π^*	$W_{\max}$	$\sigma_{x\max}$	$\sigma_{xy\ \max}$
Elastoplastic bicubic Hermite solution					
1×1	4	−248	0.196	−34900	−19200
2×2	16	−252	0.196	−34300	−19200
3×3	36	−253	0.197	−34200	−19100
4×4	64	−255	0.198	−34100	−19100
Elastoplastic bicubic spline solution					
1×1	4	−248	0.196	−34900	−19200
2×2	9	−252	0.196	−34400	−19200
3×3	16	−253	0.197	−34300	−19200
4×4	25	−255	0.198	−34100	−19200

Conclusions

The results obtained for elastic and elastoplastic plate bending problems demonstrate that accurate stresses as well as displacements are possible with a discrete element displacement formulation. The ability of bivariate Hermite displacement functions to approximate closely the derivatives of the displacement field[17] is the basis for this stress accuracy. Significantly the use of spline constraints to achieve curvature continuity does not improve the mean stress error nor does it increase the mean displacement error. Since the spline constraints reduce the number of degrees of freedom by almost a factor of four, this can be computationally quite important in linear problems when direct methods are used to solve the equilibrium equations. However, this advantage is greatly reduced when the conjugate gradient method is used because the algorithm converges in about the same number of cycles for the Hermite and spline cases. Also in nonlinear problems the re-evaluation of the element matrices for each iterate, X_i dominates the computational effort and there is even less difference. If the variable metric algorithm were used, then the smaller dimension of the metric would favor the use of spline constraints even in nonlinear problems.

The elastoplastic solutions obtained for a linear strain hardening material show that elastic compressibility has a significant influence on the stress distribution in the four corners. This is predictable from an elastic analysis but it also carries over well into the plastic range. When the slope of the linear strain hardening is small, as in the present problem, the influence dies out at high load levels. Comparisons with an incremental theory solution[4] for an elastic-perfectly plastic material show reasonable agreement for load deflection behavior. This result is not too surprising since Ohashi and Kamiya[19] had previously obtained excellent agreement between a deformation theory and experiment for a circular plate. Finally, it should be noted that the present discretization is equally applicable to an incremental theory and in fact is quite similar to the discretization used by Armen, Pifko, and Levine.

References

[1] Bogner, F. K., "Finite Deflection Discrete Element Analysis of Shells," AFFDL-TR-67-185, 1968, Wright-Patterson Air Force Base, Ohio.

[2] Fox, R. L. and Stanton, E. L., "Developments in Structural Analysis by Direct Energy Minimization," *AIAA Journal*, Vol. 6, No. 6, June 1968, pp. 1036–1042.

[3] Illyushin, A. A., *Plasticity*, Eyrolles, Paris, 1956, Chaps. 2 and 4 (in French).

[4] Armen, H., Pifko, A., and Levine, H. S., "A Finite Element Method for the Plastic Bending Analysis of Structures," *Proceedings of the Second Air Force Conference on Matrix Methods in Structural Mechanics*, Wright-Patterson Air Force Base, Ohio, 1968.

[5] Mendelson, A., *Plasticity Theory and Application*, Macmillan, New York, 1968, Chap. 7.

[6] Drucker, D. C., "A More Fundamental Approach to Plastic Stress Strain Relations," *Proceedings of the First U.S. National Congress of Applied Mechanics*, 1951, pp. 487–491.

[7] Lin, T. H., *Theory of Inelastic Structures*, Wiley, New York, 1968, Chap. 4.

[8] Budiansky, B., "A Reassessment of Deformation Theories of Plasticity," *Journal of Applied Mechanics*, Vol. 26, 1959, pp. 259–264.

[9] Havner, K. S., "On the Formulation and Iterative Solution of Small Strain Plasticity Problems," *Quarterly of Applied Mathematics*, Vol. 23, 1966, pp. 323–335.

[10] Stanton, E. L., "A Discrete Element Analysis of Elastoplastic Plates by Energy Minimization," Ph.D. thesis, 1968, Case Western Reserve Univ., Cleveland, Ohio.

[11] Mikhlin, S. G., *Variational Methods in Mathematical Physics*, Macmillan, New York, 1964, Chap. 2.

[12] Melosh, R. J., "Basis for Derivation of Matrices for the Direct Stiffness Method," *AIAA Journal*, Vol. 1, No. 7, July 1963, pp. 1631–1637.

[13] Bogner, F. K., Fox, R. L., and Schmit, L. A., "The Generation of Interelement Compatible Stiffness and Mass Matrices by the Use of Interpolation Formulas," AFFDL-TR-66-80, 1966, Wright-Patterson Air Force Base, Ohio, pp. 397–443.

[14] Tong, P. and Pian, T. H. H., "The Convergence of Finite Element Method in Solving Linear Elastic Problems," *International Journal of Solids and Structures*, Vol. 3, 1967, pp. 865–879.

[15] McLay, R. W., "Completeness and Convergence Properties of Finite Element Displacement Functions—A General Treatment," AIAA Paper 67-143, New York, 1967.

[16] Kantorovich, L. V. and Krylov, V. I., *Approximate Methods of Higher Analysis*, Noordhoff, Groningen, The Netherlands, 1958, Chap. 4.

[17] Birkhoff, G., Schultz, M. H., and Varga, R. S., "Piecewise Hermite Interpolation in One and Two Variables with Applications to Partial Differential Equations," *Numerische Mathematik*, Vol. 11, 1968, pp. 232–256.

[18] Herbold, R. J., "Consistent Quadrature Schemes for the Numerical Solution of Boundary Value Problems by Variational Techniques," Ph.D. dissertation, 1968, Case Western Reserve Univ., Cleveland, Ohio.

[19] Ohashi, Y. and Kamiya, N., "On the Bending of Thin Plates of Material Having a Nonlinear Stress Strain Relation," *International Journal of Mechanical Sciences*, Vol. 9, 1967, pp. 183–193.

[20] De Boor, C., "Bicubic Spline Interpolation," *Journal of Mathematics and Physics*, Vol. 41, 1962, pp. 212–218.

[21] Birkhoff, G. and De Boor C., "Piecewise Polynomial Interpolation and Approximation," *Approximation of Functions*, edited by H. L. Garabedian, Elsevier, New York, 1965, pp. 164–190.

[22] Schmit, L. A. et. al., "Developments in Discrete Element Finite Deflection Structural Analysis by Function Minimization," AFFDL-TR-68-126, 1968, Wright-Patterson Air Force Base, Ohio.

[23] Myers, G. E., "Properties of the Conjugate-Gradient and Davidon Methods," *Journal of Optimization Theory and Applications*, Vol. 2, 1968, pp. 209–219.

[24] Daniel, J. W., "The Conjugate Gradient Method for Linear and Nonlinear Operator Equations," *SIAM Journal of Numerical Analysis*, Vol. 4, 1967, pp. 10–26.